The Authors wish to thank the two anonymous referees for the extended review of the discussion paper "Paleoclimate in continental northwestern Europe during the Eemian and Early-Weichselian (125-97 ka): insights from a Belgian speleothem" by Vansteenberge et al.

The general comments and technical corrections made by the reviewers will be taken into account when preparing the final version of the manuscript. In this reply, the authors would like to seize the opportunity to give additional information and corrections to certain issues suggested by the reviewers.

1. Age Model

To construct the age model, the StalAge algorithm of Scholz and Hoffmann (2011) was used. Although not mentioned in the original manuscript, the three growth phases were modeled separately, as suggested by reviewer #2. This appeared the best solution to handle the occurrence of the two hiatuses. Of course, we would like to stress that each model is an interpretation. Other algorithms such as COPRA are available and could give a solution to some of the issues encountered here, however, it could potentially create others. Originally, we experimented with MOD-AGE (Hercman and Pawlak, 2012) and COPRA (Breitenbach et al., 2012). With MOD-AGE, we encountered problems with the hiatuses. In the case of COPRA, the authors are not convinced of the idea of transferring age model uncertainties to uncertainties in the proxy values. Despite some caveats, the authors are still satisfied with the performance of StalAge in this study. Also, a comparison of different age models lies beyond the scope of this paper.

We improved figure 5 with the suggestions made by both reviewers, i.e. we added labels to the data points, included the growth rate and made a clear indication of the growth phases and hiatuses.

1.1 DAT-1 and the 125.3 – 117.3 ka interval

Reviewer #1 commented that DAT-1 is excluded from the age model, although it is in stratigraphic order. It is clear that DAT-1 has only limited weight in the actual model and an explanation for this can be found in the algorithm specifications (Scholz and Hoffmann, 2011). During the modeling process, the StalAge algorithm has a step where the data is screened for the occurrence of minor outliers and age inversions. This is done by fitting error weighted straight lines through subsets of three adjacent data points (Fig. 4 in Scholz and Hoffmann, 2011). However, DAT-1 is located in the basal part of the stalagmite, so less subsets of three data points can be used including DAT-1. If DAT-1 does not fit on the error weighted straight line created with the adjacent datapoints DAT-10 and DAT-11, which is the case here, the error of DAT-1 will be increased and the weight of DAT-1 in the Monte Carlo simulation for the age fitting will decrease. This results in less solutions where DAT-1 is included in the Monte Carlo simulated age models. The occurrence of substantial changes in growth rate in the boundary areas of a speleothem sample is recognized as a limitation of the StalAge algorithm (Scholz and Hoffmann, 2011).

1.2 DAT-19 and the start of the second hiatus (H2)

The StalAge model did not incorporate the DAT-19 date. This is again caused by the fact that DAT-19 is a date located in the boundary area of the stalagmite (it is the uppermost date of growth phase 2),

since the three growth phases were modeled separately. Here, we are convinced that DAT-19 should be included, as the stalagmite petrography shows clear evidence of a significantly decreased growth rate after DAT-16 (110.6 ka), i.e. very dense, brownish calcite with fine laminae. Also, a thin section showed smaller crystals. In complex cases, such as in this study where multiple hiatuses occur, the simplest model is still the best. Therefore, we believe that linear interpolation combined with good observations of changes in petrography, is a correct way to include DAT-19.

1.3 Growth phase 3

We agree with reviewer #2 that growth phase 3 has a bad dating potential. We already limited the interpretation of this growth phase in the original manuscript, but it is now clear to us that due to this bad chronology we should restrict the paleoclimate interpretation in this manuscript to the first two growth phases. That is why we also left out the stable isotope data of growth phase 3 in figure 7.

2. Correlation test of $\delta^{13}C$ and $\delta^{18}O$

As suggested by the second review, an additional test for correlation of $\delta^{13}C$ and $\delta^{18}O$ was done by calculating the Pearson's coefficient on the entire record and on the three growth phases separately (Table 1). However, we have to be careful because a correlation between $\delta^{13}C$ and $\delta^{18}O$ does not give conclusive evidence for the presence of kinetic fractionation, as both $\delta^{13}C$ and $\delta^{18}O$ are expected to be controlled by climate and could therefore show positive or negative covariation (Dorale and Lu, 2009). The Pearson's coefficients reveal that there is a clear difference between the separate growth phases. The first growth phase, with $\rho = 0.024$, marks no covariation. The second growth phase, with $\rho = -0.467$, has a substantial degree of negative correlation, whereas the third growth phase ($\rho = 0.461$) has a positive correlation. We believe that the difference between the correlation coefficients of the separate growth phases indicate that different processes are controlling the stable isotope variability, and that the presence or absence of covariation reflects changes in climate conditions between the growth phases rather than the presence or absence of equilibrium.

3. Control on stable isotope variations in Han-9

We agree with both reviewers that the discussion of the processes controlling the stable isotope variations in Han-9 is unclear and should be rewritten. Also, additional measurements of recent calcite were done to improve the understanding of the stable isotope functioning of the cave environment. Three samples of recent calcite were harvested by scraping off speleothem calcite from the tip of actively growing speleothems near the sample site of Han-9. The results are displayed in table 2.

3.1 $\delta^{13}C$

The $\delta^{13}C$ in Han-9 is controlled by changes in vegetation assembly above the cave. This is deduced from the match between Han-9 $\delta^{13}C$ and the abundance of grass pollen in the assembly of Sirocko et al. (2005) recovered from the Eifel maar. The agreement between Han-9 $\delta^{13}C$ and the Eifel pollen assembly is remarkable; increases in $\delta^{13}C$ occur when the percentage of grass pollen increases in the Eifel record. Also, the $\delta^{13}C$ of recent calcite formed with a current forest-type vegetation cover above the cave is ~-8‰. These values are similar to those observed during the last interglacial in Han-9 (125.3-117.3 ka). In the original manuscript it is stated that changes in C3-C4 vegetation types control the $\delta^{13}C$ variability in Han-9. We have to recall this statement because a higher abundance of grasses

does not necessarily result in an increased amount of C4 vegetation. First of all, C4 species make up only 1% of the total amount of vascular plant species in northwestern Europe today (Pyankov et al., 2010). Secondly, C4 species dominantly occur in a warmer, tropical climate (Ehleringer et al., 1997). Finally, within the subfamily of the Poideae, commonly referred to as the cool-season grasses and thriving in temperate European climate, all species use the C3 pathway (Soreng et al., 2015). The reason why speleothem calcite tends to be enriched in ^{13}C when vegetation is dominated by grasses is because grasses have a smaller biomass than trees and also the amount of soil respiration is lower, both leading to a smaller fraction of biogenic CO_2 compared to (heavier) atmospheric CO_2 within the soil (Genty et al., 2003). The similarity between the two records does not seem to hold up after 109 ka. From here on, $\delta^{13}C$ becomes more depleted while Eifel record shifts towards an assembly dominated by grasses. This is especially the case after 106 ka, when grass pollen make up to 60% of the total assembly and where the most depleted values of $\delta^{13}C$, between -9 and -10‰, occur. These are even lower than the recent calcite $\delta^{13}C$ values of ~-8‰. It is not clear to us what might have caused this depletion.

Prior calcite precipitation (PCP) is believed to control seasonal variations in the $\delta^{13}C$ of Han-sur-Lesse speleothems, as concluded from an elaborate cave monitoring study by Van Rampelbergh et al. (2014). However, the study by Van Rampelbergh et al. (2014) was carried out on a large, tabular-shaped stalagmite with drip water discharge rates of 300mL min^{-1} and growth rates of ~1mm yr^{-1}, so caution is required when extrapolating these cave monitoring conclusions to smaller, slower growing stalagmites in a different part of the cave system. If PCP occurs at one site in the cave, it does not mean that it occurs over the entire cave (Riechelmann et al., 2011). Since no additional data on Sr and Mg is currently available for Han-9, the presence of PCP cannot be confirmed, neither rejected.

To conclude, the control on Han-9 $\delta^{13}C$ is the amount of biogenic CO_2 in the soil, caused by changes in the vegetation type above the cave (forest/grasses) and thus directly linked to climate. Lower, depleted $\delta^{13}C$ values occur during warmer and wetter periods, when vegetation is dominated by temperate trees. Higher, enriched $\delta^{13}C$ values of speleothem calcite correspond with a higher abundance of grasses above the cave during colder/dryer climate intervals.

3.2 $\delta^{18}O$

The $\delta^{18}O$ variations in Han-9 are believed to reflect the temperature change, which controls the rainwater $\delta^{18}O$ through temperature dependent fractionation on the vapor condensation in the atmosphere. Lower temperatures leads to more negative rainwater $\delta^{18}O$ which is then reflected in the speleothem $\delta^{18}O$. This relation is clear in growth phase 2, where more positive $\delta^{13}C$ values, which are known to reflect lower temperatures through vegetation changes, correspond with more negative $\delta^{18}O$. This is also reflected in the strong negative correlation (Table 1). However, this does not explain the increase in $\delta^{18}O$ starting at 120 ka, as we would expect a decrease of temperature here. An increase in $\delta^{18}O$ caused by a growing ice-sheet is a plausible explanation, as sea level reconstructions also indicated that regression, caused by ice build-up, started at that time (Hearty et al., 2007). During growth phase 2, temperature drops significantly, leading to a lower $\delta^{18}O$ which cancels out the ice build-up effect.

Response to minor comments

Line 70: gradual cooling of the general climate state.

Line 95: The Han-9 was deliberately sampled because it had fallen over and was already broken into three parts. In this way, no other speleothems had to be destroyed. The speleothem was in-situ, no signs of transport near the sample site were observed.

Line 108: There is no distinct seasonal trend in the amount of rainfall over a year. The dominant moisture source in northwestern Europe is the subtropical North-Atlantic Ocean, and this remains constant throughout the year (Gimeno, 2010). The modern $\delta^{18}O$ of rainfall above the cave was monitored by Van Rampelbergh et al. (2014) over the entire year 2013 and seasonally varied between -17‰ in winter and -4‰ in summer.

Line 115: Flooding does not affect the sampling site.

Line 120: Temperature logging took place in the Réseau Renversé and sampling interval was 2 hours.

Line 121: The average temperature for the 1999-2013 period is 10.2°C, which is 1°C higher than the average temperature for 2013. The logging shows that the cave temperature is constant through the year and that the cave environment is sensitive to changes in the average temperature above the cave.

There is no evidence for any changes in the morphology of the Réseau Renversé since the last interglacial.

Line 138: The $^{230}Th/^{232}Th$ atomic ratio.

Line 139: The age datum is 1950 CE.

Line 142: Stable isotopes were measured in the Stable Isotope Laboratory at the Vrije Universiteit Brussel.

Line 144: Tungsten carbide drill bits with a diameter of 300µm were used.

Line 146: Samples were kept at 50°C prior to analysis to avoid contamination with atmospheric water vapor.

Line 149: The MAR-2 standard consists of Marbella Limestone.

Line 153: Every eight samples a replicate was measured in a different batch to check the reproducibility of the analytical method.

Line 154: A point was identified as an outlier if the difference of the value and the average of 10 previous and 10 following points was higher than two standard deviations of the 20 adjacent points.

Line 167: The discontinuities were identified macroscopically. Later on, these two discontinuities were attributed to hiatuses based on the ages.

Line 174: No internal layering is visible macroscopically.

Line 183: The smaller, equant calcite crystals occur between 200 and 176mm dft and are then followed by a fine layer of brown detrital material representing D2.

Line 185: Samples were pretty clean, as the detrital Th content, estimated by ^{232}Th concentration and an initial $^{230}Th/^{232}Th$ ratio of 4.4 ±2.2 $x10^{-6}$, is relatively low in all samples (range 6419 – 208 ppt). This leads to only minor corrections for the ^{230}Th age (table 1 in original manuscript).

Line 198: Larger amplitude variations in $\delta^{13}C$ and $\delta^{18}O$ are present between 300 and 170mm dft. This is the speleothem section in between the two discontinuities and it is characterized by abrupt changes between dense, darker calcite and coarse, whiter calcite.

Line 199: Equilibrium deposition in Han-sur-Lesse Cave was observed by Van Rampelbergh et al. (2014).

Line 224-232: The temporal sampling interval was calculated based on the age model. The largest sampling interval is ~100 years, occurring just before Hiatus 2. The smallest interval is 0.3 years, which is located before Hiatus 1, between 330 and 320mm dft (growth rate curve in Fig. 5).

Line 291: The title “A late onset of the Eemian” is indeed misleading, as it is clear from other records and Han-9 as well that Eemian interglacial conditions were already present when the speleothem started growing.

Line 316-317: At the start of Han-9 growth, $\delta^{13}C$ is depleted with values up to -9‰. Such depleted values are indicative for vegetation dominated by trees above the cave. This is also evidenced by the abundance of tree pollen in the Eifel record. Because of this forest type vegetation it is assumed that, in terms of temperature, interglacial conditions were already present before 125 ka.

Line 333: There are no changes in the morphology of the speleothem in between 125 and 120 ka, i.e. there is well-expressed layered calcite with constant layer thickness. It is believed that this is caused by absence of distinctive changes in temperature/water availability, as it corresponds to the period where the stable isotopes also show the smallest variations.

Line 355: Nothing happens as a result of the $\delta^{13}C$ increase, it is the enrichment in ^{13}C itself that is the result of an increase in grass-type vegetation caused by a drying/cooling event between 117.5 and 117.3 ka. Boreal forests do recover after the LEAP event, but the speleothem doesn’t start growing until much later. A similar observation is made for the start of the speleothem growth at 125.3 ka: interglacial conditions were already present, yet the speleothem growth did not start immediately. It is not clear whether this is a site-specific effect or controlled by climate, but in the latter we could hypothesize that climate conditions need to be more favorable to initiate speleothem growth than to sustain it.

Line 396: The variability in the $\delta^{13}C$ and $\delta^{18}O$ between 112.9 and 111 ka is mainly temperature controlled: 1) lower temperatures lead to more negative $\delta^{18}O$ values and 2) during colder periods grasses are more abundant causing an increase in $\delta^{13}C$. This negative correlation of $\delta^{13}C$ and $\delta^{18}O$ is reflected in the Pearson’s correlation coefficient of -0.467.

Figure 5 is updated with the suggestions made by both reviewers.

Figure 7: As suggested by reviewer #2, we added three additional datasets to figure 7:

- MD03-2664 planktonic $\delta^{18}O$ record (Irvali et al., 2012)
- Asian monsoon speleothem $\delta^{18}O$ record (Yuan et al., 2004)

- TKS flowstone $\delta^{18}O$ (Meyer et al., 2008).

Axis of Han-9 $\delta^{13}C$ and $\delta^{18}O$ were enlarged, insolation curve moved closer to Han-9 stable isotope data, U/Th data axis adjusted. Speleothem records from the Alps were plot on a single axis. MIS5e and 5d subdivision was added. Also, the climatic intervals identified in Han-9 are now displayed in the figure. Arrows indicating control on stable isotope changes were added.

Additional references

Breitenbach, S. F. M., Rehfeld, K., Goswami, B., Baldini, J. U. L., Ridley, H. E., Kennett, D. J., Prufer, K. M., Aquino, V. V., Asmerom, Y., Polyak, V. J., Cheng, H., Kurths, J., Marwan, N.: Constructing Proxy Records from Age models (COPRA), Climate of the Past, 8, 1765-1779, 2012.

Dorale, J. A., Liu, Z.: Limitations of Hendy test criteria in judging the paleoclimatic suitability of speleothems and the need for replication, Journal of Cave and Karst Studies, 71, 73-80, 2009.

Ehleringer, J. E., Cerling, T. E., Helliker, B. R., C4 photoynthesis, atmospheric CO2, and climate, Oecologia, 112, 285-299, 1997.

Gimeno, L., Drumond, A., Nieto, R., Trigo, R. M., Stohl, A.: On the origin of continental precipitation, Geophysical Research Letters, 37, L13804, doi:10.1029/2010GL043712, 2010.

Hercman, H., Pawlak, J.: MOD-AGE: an age-depth model construction algorithm, Quaternary Geochronology, 12, 1-10, 2012.

Pyankov, V. I., Ziegler, H., Akhani, H., Deigele, C., Lüttge, U.: European plants with C4 photosynthesis: geographical and taxonomic distribution and relations to climate parameters, Botanical Journal of the Linnean Society, 163, 283-304, 2010.

Riechelmann, D. F. C., Schroeder-Ritzrau, A., Scholz, D., Fohlmeister, J., Spoetl, C., Richter, D. K., Mangini, A.: Monitoring Bunker Cave (NW Germany): A prerequisite to interpret geochemical proxy data of speleothems from this site, Journal of Hydrology, 409, 682-695, 2011.

Soreng, R. J., Peterson, P. M., Romaschenko, K., Davidse, G., Zuloaga, F. O., Judziewicz, E. J., Filguieras, T. S., Davis, J. I., Morrone, O.: A worldwide phylogenetic classification of the Poaceae (Gramineae), Journal of Systematics and Evolution, 53(2), 117-137, 2015.

Yuan, D., Cheng, H., Edwards, R. L., Dykoski, C. A., Kelly, M. J., Zhang, M., Qing, J., Lin, Y., Wang, Y., Wu, J., Dorale, J., An, Z., Cai, Y.: Timing, Durqtion and Transition of the Last Interglacial Asian Monsoon, Science, 304, 575-578, 2004.

	ρ	# measurements
GP1	0,024	599
GP2	-0,467	235
GP3	0,461	284
Total	-0,197	1118

Table 1: Pearson's coefficient of correlation (ρ) calculated for the three growth phases and for the total record.

	$\delta^{13}C$	$\delta^{18}O$
RC1	-8,19	-5,73
RC2	-8,20	-6,25
RC3	-7,80	-6,48

Table 2: $\delta^{13}C$ and $\delta^{18}O$ analysis of three recent calcite samples from the Réseau Renversé.

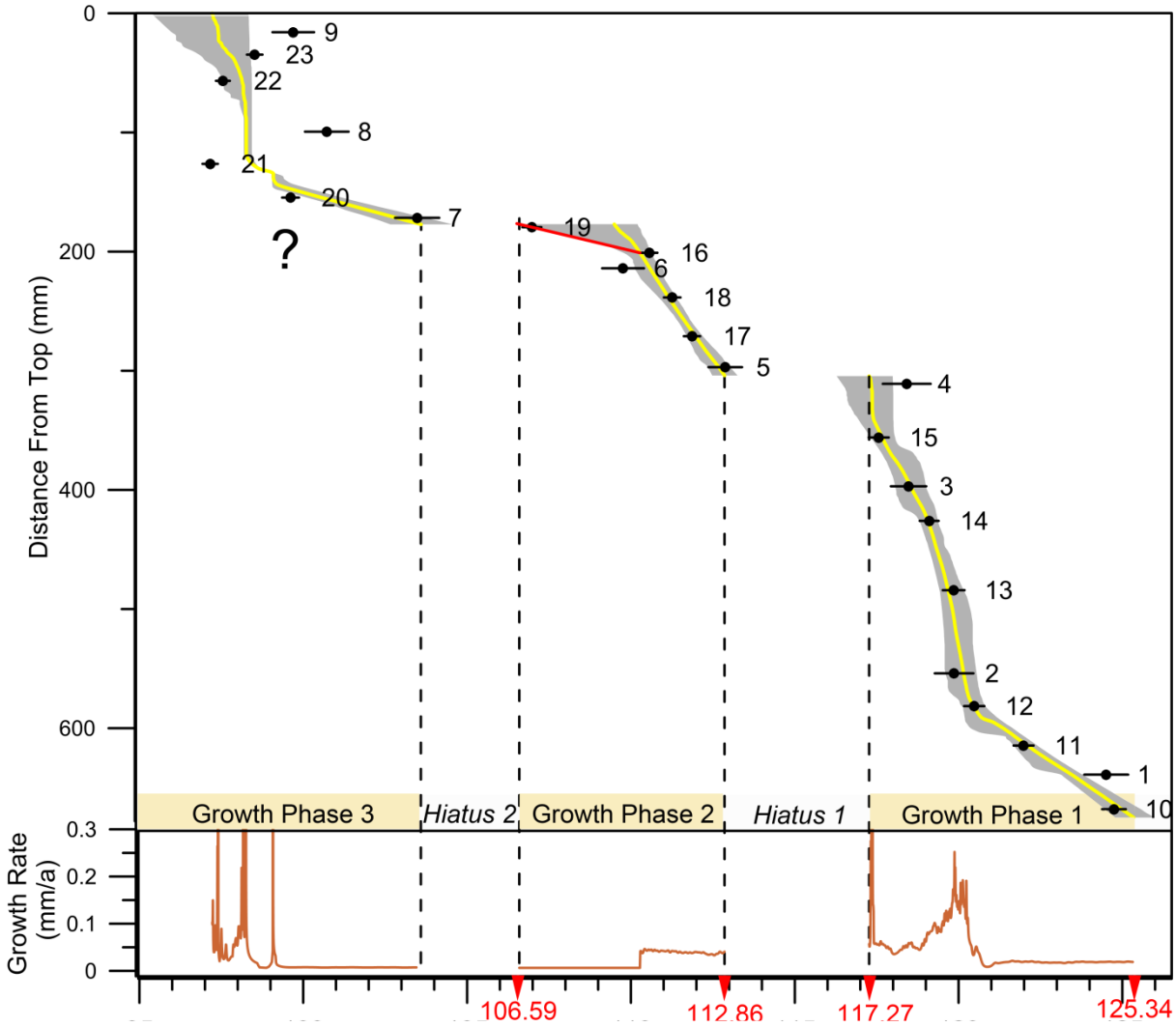

Figure 5 revised: Han-9 age-depth model constructed with the StalAge algorithm (Scholz and Hoffmann, 2011). The actual age-depth model is represented by the yellow line, the grey area marks the error. Numbers represent the sample labels (Table 1 in original manuscript). The brown curve displays the growth rate. Numbers in red indicate important dates and are discussed in the text.

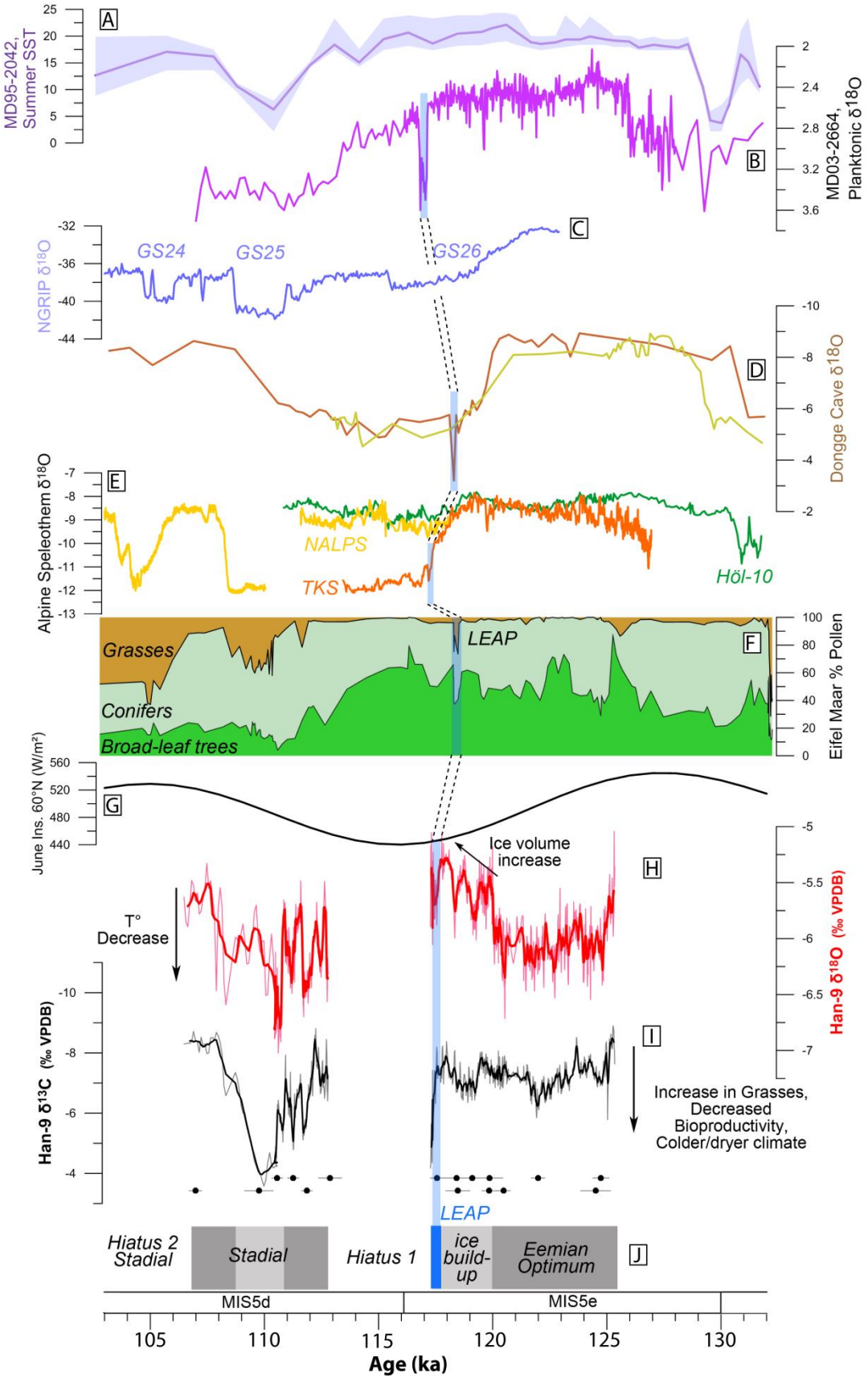
A
MD95-2042, Summer SST
B
MD03-2664, Planktonic δ18O
C
NGRIP δ18O
GS24
GS25
GS26
D
Dongge Cave δ18O
E
Alpine Speleothem δ18O
NALPS
TKS
Höl-10
F
Grasses
Conifers
Broad-leaf trees
LEAP
Eifel Maar % Pollen
G
June Ins. 60°N (W/m²)
H
Ice volume increase
T° Decrease
Han-9 δ18O (‰ VPDB)
I
Han-9 δ13C (‰ VPDB)
Increase in Grasses, Decreased Bioproductivity, Colder/dryer climate
LEAP
J
Hiatus 2
Stadial
Stadial
Hiatus 1
ice build-up
Eemian Optimum
MIS5d
MIS5e
Age (ka)

Figure 7 revised: Comparison of Han-9 stalagmite with other records. The shaded blue area marks the occurrence of the Late Eemian Aridity Pulse (LEAP) in the Eifel record and its equivalent in other records. **A)** Sea Surface Temperature (SST) reconstruction from marine core MD04-2845 (Sanchez-Goñi et al., 2012); **B)** Planktonic $\delta^{18}O$ from marine core MD03-2664 (Irvali et al., 2012); **C)** NGRIP $\delta^{18}O$ record with indication of Greenland Stadial intervals (NGRIP members, 2004); **D)** Asian monsoon reconstructions from Dongge Cave (D3 & D4 stalagmites; Yuan et al., 2004); **E)** Alpine speleothem $\delta^{18}O$ (TKS: Meyer et al., 2008; NALPS: Boch et al., 2011; HöL-10: Moseley et al., 2015)**; F)** Eifel Maar pollen assembly (Sirocko et al., 2005); **G)** June insolation for 60°N (Berger and Loutre, 1991); **H)** & **I)** Han-9 stable isotope record with a 7-point moving average and U/Th dates; **J)** Paleoclimate interpretation of Han-9.